Special Issue

Local Progression Kinetics of Geographic Atrophy in Age-Related Macular Degeneration Are Associated With Atrophy Border Morphology

Moritz Lindner,[1–3] Sebastian Kosanetzky,[1] Maximilian Pfau,[1] Jennifer Nadal,[4] Lukas A. Gördt,[1] Steffen Schmitz-Valckenberg,[1] Matthias Schmid,[4] Frank G. Holz,[1] and Monika Fleckenstein[1]; for the FAM-Study Group

[1]Department of Ophthalmology, University of Bonn, Bonn, Germany
[2]The Nuffield Laboratory of Ophthalmology, Sleep and Circadian Neuroscience Institute, Nuffield Department of Clinical Neurosciences, University of Oxford, Oxford, United Kingdom
[3]Oxford Eye Hospital, Oxford University Hospitals NHS Foundation Trust, Oxford, United Kingdom
[4]Institute for Medical Biometry, Informatics and Epidemiology, University Hospital Bonn, Bonn, Germany

Correspondence: Monika Fleckenstein, Department of Ophthalmology, University of Bonn, Ernst-Abbe-Str. 2, 53127 Bonn, Germany; Monika.Fleckenstein@ukbonn.de.

See the appendix for the members of the FAM-Study Group.

Submitted: October 22, 2017
Accepted: January 29, 2018

Citation: Lindner M, Kosanetzky S, Pfau M, et al.; for the FAM-Study Group. Local progression kinetics of geographic atrophy in age-related macular degeneration are associated with atrophy border morphology. *Invest. Ophthalmol Vis Sci*. 2018;59:AMD12–AMD18. https://doi.org/10.1167/iovs.17-23203

Purpose. To assess the impact of distinct atrophy border characteristics based on spectral-domain optical coherence tomography (SD-OCT) imaging on local atrophy progression.

Methods. Patients with geographic atrophy (GA) secondary to AMD were recruited in the context of the Longitudinal Fundus Autofluorescence in Age-related Macular Degeneration and Directional Spread in Geographic Atrophy studies (NCT00393692, NCT02051998). Horizontal and vertical SD-OCT scans were acquired at sequential visits using a device allowing for anatomically accurate registration of follow-up to baseline scans. For quantification of local atrophy progression, the lateral spread of GA (LSGA) was measured. Further, border types were independently graded. Comparison of LSGA between the different border types was performed using linear mixed-effects models.

Results. Seventy-two eyes of 49 patients (27 female) aged 74.0 years (Inter quartile range [IQR], 68.1–79.0) were included into this analysis. A total of 258 border sections were analyzed longitudinally over a median period of 1.2 years (IQR, 0.9–1.6). At baseline, 17.1% borders were classified as 'regular', 47.7% as 'irregular', and 35.3% as 'splitting'. Sixty-two percent of the eyes exhibited more than one border type. LSGA was slowest in 'regular' borders (62.85 ± 25.29 μm/y), followed by 'irregular' borders (91.15 ± 15.05 μm/y) and fastest in 'splitting' borders (183.15 ± 18.17 μm/y). Differences between the 'splitting' and each other border type were statistically significant ($P < 0.001$).

Conclusions. The results indicate that SD-OCT–based assessment of local GA border morphology can serve as a predictor for local atrophy progression. These observations help to better understand the natural history and potential pathogenetic factors of GA development and progression.

Keywords: optical coherence tomography, geographic atrophy, age-related macular degeneration

Geographic atrophy (GA) represents the late-stage of nonexudative AMD.[1–3] It is present in 3.5% of people over 75 years [4,5] and becomes the predominant type of late AMD in the population of 85 years and older.[6] In industrial countries, late stage neovascular or dry AMD is the leading cause of legal blindness in the elderly.[7–9] Although the exact pathogenetic mechanisms leading to GA are still poorly understood, chronic inflammatory processes, excessive lipofuscin accumulation in the retinal pigment epithelium (RPE) lysosomal compartment, complement system dysregulation, and vascular factors have been implicated in the development of AMD (reviewed in Ref. 10). In contrast to neovascular AMD, there is yet no therapy available for patients with GA. Therapeutic trials for GA currently emerge. The capacity of future therapeutic trials to detect drug efficacy depends on sensitive and reliable outcome measures as well as on refined cohort stratification.

Histologically, areas of GA are characterized by degeneration of the RPE, of outer layers of the neurosensory retina, and the choriocapillaris.[11,12] Cross-sectional in vivo visualization of the morphology of the retina and the RPE–Bruch's membrane (BM) complex has become possible by the advent of spectral-domain optical coherence tomography (SD-OCT).[13–15] The border zone of atrophy represents the area where pathologic processes promote atrophy progression and has, therefore, recently received major attention.[16–21] Brar et al.[19] originally identified two distinct types of atrophy border: type 1 (also termed 'regular' according to Fleckenstein et al.,[18] Fig. 1A) shows smooth margins and no alterations of the outer retina while type 2 (also termed 'irregular',[18] Fig. 1B) exhibits severe alterations in the outer retinal layers and irregular margins occasionally with increased optical reflectivity of the RPE. Subsequently, we have identified a third atrophy border type,

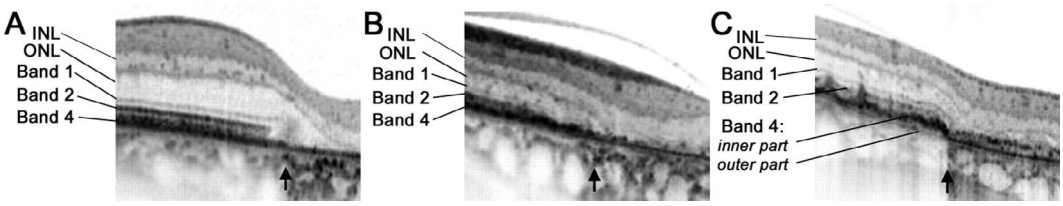

Figure 1. Different types of borders as visualized by SD-OCT. (**A**, **B**) The assumed RPE–BM complex (band 4) narrows, and an outer layer remains throughout the atrophic area (assumed BM). The margin depicted in (**A**) represents a 'regular'[18] or 'type 1'[18,19] border with smooth margins and no alterations of the outer retina. The margin in (**B**) represents an 'irregular'[18] or 'type 2'[19] border with severe alterations in the outer retinal layers and irregular margins. (**C**) The 'splitting' border[18] characterized by splitting of the RPE–BM complex in inner and outer regions. Image obtained from Ref. 18. INL, inner nuclear layer; ONL, outer nuclear layer; band 1, external limiting membrane; band 2, ellipsoid zone; band 4, RPE–BM complex.

termed 'splitting' (Fig. 1C).[18] This border type is characterized by an obvious separation of the RPE–BM complex. It has been speculated that the origin of this separation is an excessive diffuse accumulation of extracellular material.[18] Though the 'splitting' border type has originally been identified in the context of a particularly fast progressing atrophy phenotype, termed 'diffuse-trickling',[18,22] it is also observed in other phenotypes of GA.[23] The 'splitting' border type has already been shown to be associated with overall more rapid atrophy progression.[23]

Studies addressing local atrophy progression are limited.[21,24,25] Yet, prediction of local atrophy progression is of particular interest to predict future involvement of distinct retinal areas, particularly the fovea. Thus, assessment of local atrophy progression could be a more meaningful predictor for visual acuity loss than overall atrophy progression. In the present substudy, we aim to analyze the prognostic value of different atrophy border types as visualized by SD-OCT imaging on local GA progression.

Methods

Patients

All subjects presented in this substudy were prospectively recruited at the Department of Ophthalmology, University of Bonn in the context of the Fundus Autofluorescence in Age-Related Macular Degeneration (FAM) study and its extension trial Directional Spread in Geographic Atrophy (DSGA) (NCT00393692, NCT02051998), both longitudinal natural history studies in patients with AMD. The FAM study was a multicenter observational study with a total of 625 patients recruited at the following centers: Department of Ophthalmology, University of Aachen, Germany; Department of Ophthalmology, University of Bonn, Germany; Department of Ophthalmology, University of Heidelberg, Germany; Department of Ophthalmology, University of Leipzig, Germany; St. Franziskus Hospital Münster, Germany; and Department of Ophthalmology, University of Würzburg, Germany. In 2007, high-resolution SD-OCT (Spectralis HRA+OCT; Heidelberg Engineering, Hedielberg, Germany) became available during the course of the study at the Department of Ophthalmology, University of Bonn and was incorporated into the study protocol. The site's ethics committee approved this protocol amendment.

The DSGA study represents the extension of the FAM study at the Department of Ophthalmology, University of Bonn. Compared with FAM, DSGA comprise additional imaging techniques as well as image analysis strategies. The inclusion and exclusion criteria for these studies have been described in detail previously.[26–28] Patients participating in FAM/DSGA at the Department of Ophthalmology, University of Bonn (n = 141 at time of data analysis) were assessed for eligibility for the current substudy if they exhibited unifocal or multifocal GA in at least one eye and SD-OCT imaging had been performed (n = 121). Exclusion criteria were past or present neovascular changes, any history of retinal surgery, laser photocoagulation, radiation therapy, or other retinal diseases in the study eye. If both eyes of a patient met the inclusion criteria, both were included in this substudy.

The study followed the tenets of the Declaration of Helsinki and was approved by the local institutional review boards and the local Ethics Committees at the participating study centers. Informed consent was obtained from each patient after explanation of the nature and possible consequences of the study.

Image Acquisition

Pupils were dilated with 1.0% tropicamide and 2.5% phenylephrine before acquisition of retinal images. High-resolution imaging was performed using a combined instrument (Spectralis HRA+OCT; Heidelberg Engineering, Heidelberg, Germany) that allows for simultaneous recording of confocal laser scanning ophthalmoscopy (cSLO) and SD-OCT images as previously described.[29,30] In all patients included in this substudy, a minimum standardized imaging protocol was performed, which included acquisition of 488-nm fundus autofluorescence (FAF) and near-infrared reflectance ($\lambda = 830$ nm; field of view, 30° × 30°; image resolution, 768 × 768 pixels) and simultaneous SD-OCT scanning using a second, independent pair of scanning mirrors ($\lambda = 870$ nm; acquisition speed, 40,000 A-scans per seconds; scan depth, 1.8 mm; digital depth resolution, ~3.5 μm per pixel).[16] This allows for real-time registration and compensation of eye movements. In each study eye, 30° vertical and horizontal SD-OCT-scans consisting of 768 A-scans were obtained in high-speed mode. The automatic real time (ART) mean function was usually set to 100. At follow-up visits all scans were obtained using the software's 'follow-up mode' that allows for anatomically registration of follow-up SD-OCT scans to the position of the scans acquired at baseline with high precision.[17,30] Only eyes with at least two examinations with good quality horizontal and vertical SD-OCT scans were included in the analysis.

Image Analysis

For each atrophic border, two independent graders analyzed two paired SD-OCT scans: one from baseline and one from the latest follow-up visit. Before evaluation of retinal changes over time, the alignment of the follow-up SD-OCT scans with the baseline images was verified by comparing the position of blood vessels. Individual bands below the hyporeflective band of the outer nuclear layer[14] were identified. For quantitative analyses, four GA borders (superior, nasal, temporal, inferior) per eye were analyzed at baseline and at latest follow-up. These were the nasal and temporal borders of the horizontal B-scan

and the inferior and superior borders of the vertical B-scan, respectively. The site of the GA border was identified at baseline and follow-up. The exact position of the border was defined as the point with an abrupt beginning of choroidal hypertransmission on the SD-OCT scan—that is, a change of the normal hyporeflective to an abnormal hyperreflective signal at the level of the choroid below BM. This hyperreflective area has been shown to spatially correlate with the severe reduction of the FAF signal over atrophy in the corresponding cSLO.[31] Furthermore, the GA phenotype was classified as 'diffuse-trickling' or 'non-diffuse-trickling' based on the perilesional FAF patterns according to Holz et al.[22,32] SD-OCT scans and FAF images were analyzed using the commercially available SD-OCT viewer and analysis software (Eye Explorer; Heidelberg Engineering).

Atrophy border types for each of the four GA border locations (superior, nasal, temporal, inferior) were classified as previously described by two independent readers.[18,19] A single GA lesion could harbor distinct GA border types, but only one single border type could be assigned per border location. Border types were classified as follows: the 'regular' border (corresponding to type 1 by Brar et al.[19]) shows smooth margins and no alterations of the outer retina; the 'irregular' border (type 2 according to Brar et al.[19]) exhibits severe alterations in the outer retinal layers and irregular margins with or without increased optical reflectivity of the RPE; the 'splitting' border is characterized by a splitting of the RPE–BM complex into two hyperreflective bands. Representative examples for each border type are given in Figure 1. Grading of local atrophy progression and of the border type of a single eye performed on different days.

For the purpose of this substudy, the GA border as visualized on SD-OCT-scans was defined as the site where choroidal hypertransmission started. Local GA progression (lateral spread of GA [LSGA]) was quantified as previously described.[17] In brief, this was realized using the green vertical line provided as location marker by the software that was positioned at the atrophy border at baseline. After switching to the last follow-up scan, the distance (in μm) between the green line and the position of the GA border was measured using the distance tool of the software and LSGA, defined as change in border position over time, was calculated. Noteworthy, the angle of incidence by which the SD-OCT scan crosses the atrophy border has a notable influence on the measured value for LSGA (see Supplementary Fig. S1 illustrating of this effect), and thereby adds variability to the data presented herein.

Eyes with valid values for border type and LSGA from less than three borders were excluded from the entire analysis (63 eyes). Invalid values for atrophy border type occurred when classification failed, for example, due to insufficient scan quality, or because the border type could not be univocally grouped into one of the three categories (99 borders, causing exclusion of 28 eyes), or a border was located outside the image frame (84 borders, causing exclusion of 36 eyes). In two eyes, a combination of the above caused exclusion and for three eyes both exclusion criteria applied. A summary of the eyes excluded from analysis is presented in Figure 2.

Statistical Analysis

Data were compiled into a spreadsheet application and analyzed using the R software for statistical computing (version 3.3.0; Vienna, Austria).[33] Dependencies between atrophy border type and border location as well as FAF pattern were assessed using the χ^2 test. Interrater agreement for grading of the border type was assessed using Cohen's kappa. Effect of atrophy border type and FAF pattern on LSGA were analyzed using a linear mixed-effects model accounting for patient- and eye-specific characteristics. The model was designed in analog to previous descriptions.[17,34] To analyze mean differences in LSGA between different border types, mixed-effects modeling was followed by the application of Tukey's honest significant difference (HSD) post hoc tests. Estimated LSGA values obtained from mixed-effects model analysis are presented as mean ± standard error (SE). All further results are presented as median (interquartile range [IQR]). $P < 0.05$ was considered significant.

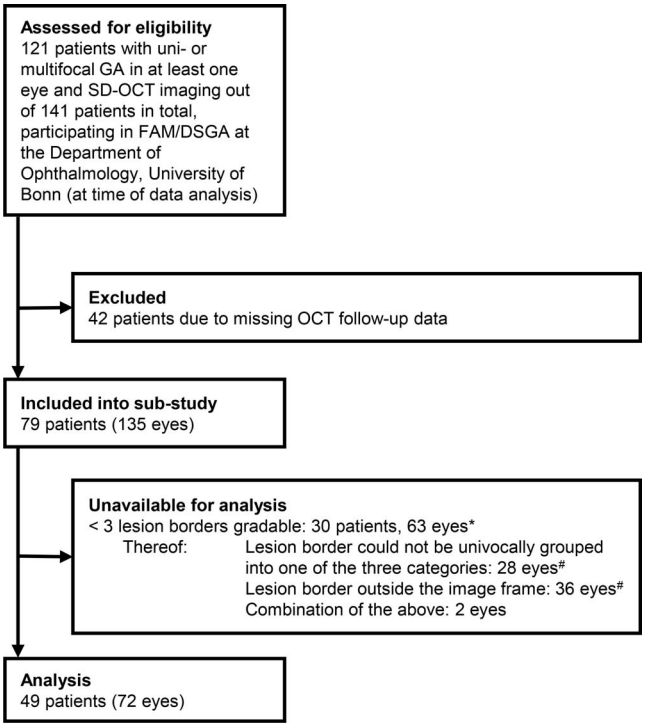

FIGURE 2. Flowchart summarizing the dropouts as a result of applying the distinct inclusion and exclusion criteria. *Number of eyes is higher than two times the number of patients because in several instances only one eye of a patient was excluded. So this patient would remain study participant with his other eye being included into the analysis. #In three eyes, both these exclusion criteria apply and they therefore appear twice.

RESULTS

At time of data analysis for the current substudy, of the 141 patients participating in the FAM and/or DSGA study at the Department of Ophthalmology, University of Bonn, a total of 121 patients exhibited unifocal or multifocal GA in at least one eye and SD-OCT imaging had been performed. These patients were assessed for eligibility for the current analysis. Of these, 49 patients (72 eyes) were included (27 female [55.1%] and 22 male [44.9%]; median age at baseline: 74.01 years [IQR, 68.12–78.98; minimum, 55.03; maximum, 90.46]). Figure 2 summarizes the reasons for exclusion. In these patients, serial SD-OCT imaging was performed over a median follow-up period of 1.19 years (IQR, 0.90–1.61; minimum, 0.50; maximum, 2.78, Supplementary Table S1). Based on baseline FAF images, 18 (25.0% eyes were graded as 'diffuse-trickling' GA while 54 (75.0%) were grade as 'non-diffuse-trickling' GA. Overall, on SD-OCT 278 atrophy borders were analyzed at both, baseline and follow-up images by two independent readers. Agreement between the two readers for grading of the border type was overall high (kappa = 0.85). At baseline, 44 (17.1%) borders

Table. Atrophy Progression (μm/y) by Border Type

Border Type	Estimated LSGA, μm/y	SE	*P* Value
Regular	62.85	22.14	<0.001
Irregular	91.15	15.05	<0.001
Splitting	183.15	18.17	<0.001

Results obtained from linear mixed-effects modeling.

were classified as 'regular', 123 (47.7%) as 'irregular', and 91 (35.2%) as 'splitting' (Supplementary Table S2). Forty-nine percent of the eyes showed at least two distinct border types. Distributions of the single border types did not differ significantly between the four border locations (i.e. superior, nasal, inferior, temporal; $P = 0.997$). Yet, distribution of atrophy borders differed significantly between eyes with 'diffuse-trickling' and 'non-diffuse-trickling' GA ($P < 0.001$). Border types were highly inert over time. Of the borders graded as 'regular' at baseline 84.4% received the same grading at follow-up. In analog, 89.5% graded as 'irregular' and 91.0% of the borders graded as splitting at baseline, received the same grading at the follow-up visit.

Overall LSGA was 117.86 ± 9.19 μm/y. According to the results of the mixed-effects model, annual LSGA was slowest in borders of the type 'regular' with 62.85 ± 25.29 μm/y. LSGA was faster by 28.29 ± 15.05 μm/y in 'irregular'-type borders and by 120.29 ± 22.76 μm/y in 'splitting'-type borders. The difference in LSGA between the three border types was significant ($P < 0.001$). Obtained progression rates are summarized in the Table. According to Tukey's HSD post hoc test, significant differences between the single border type were present between 'splitting' and 'irregular' as well as the 'splitting' and 'regular' ($P < 0.001$ each) borders, but not between 'regular' and 'irregular' ($P = 0.487$) borders. As border type distribution was significantly different between 'diffuse-trickling' and 'non-diffuse-trickling' eyes, an additional model was fitted including the FAF pattern as a fixed effect. Herein, the OCT border type was still significantly associated with LSGA ($P < 0.001$, Fig. 3).

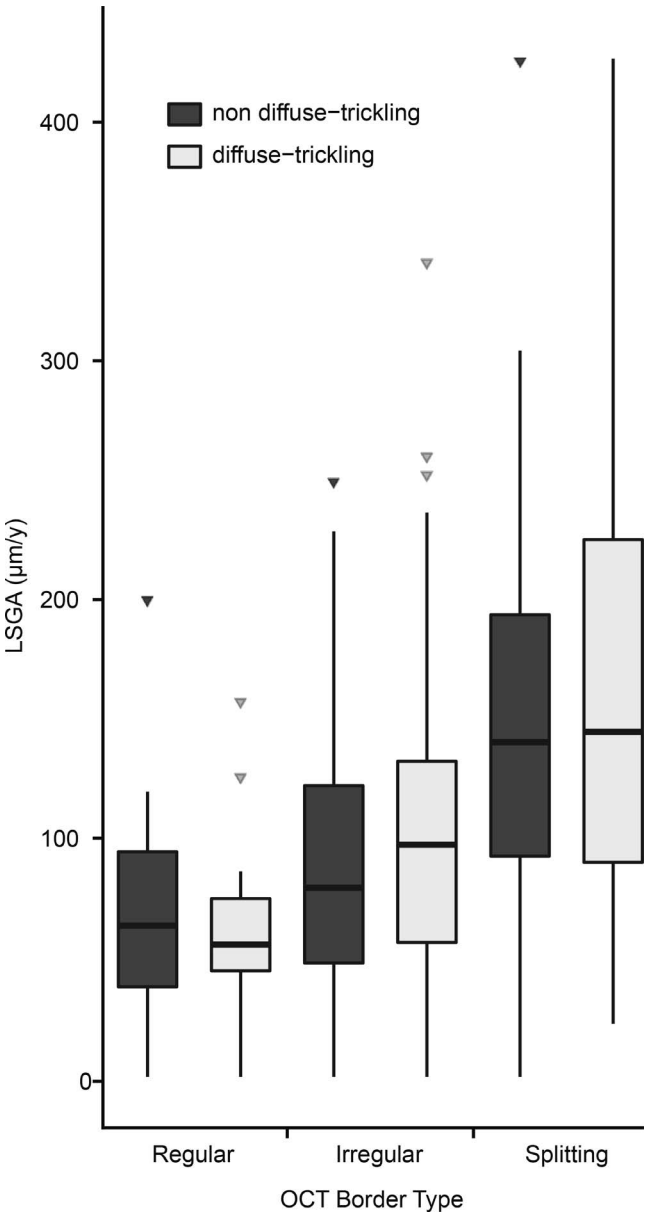

Figure 3. LSGA for the border types ('regular', 'irregular', and 'splitting') as visualized using SD-OCT. Results are presented separately for 'diffuse-trickling' and 'non-diffuse-trickling' lesions.

Discussion

The results demonstrate relevance of morphologically distinct GA border types as visualized by SD-OCT imaging for local atrophy enlargement over time. Difference in atrophy progression was assessed using a linear mixed-effects model particularly showing that the presence of the 'splitting' border type was associated with a significantly faster lateral progression of the atrophic lesion (LSGA). To account for the previously reported faster overall atrophy progression and the high frequency of 'splitting' borders in the 'diffuse-trickling' FAF phenotype,[18] an additional model with a term for the FAF pattern was created. Herein, the 'splitting' border type still accounted with a significantly faster LSGA.

The underlying biologic processes driving the distinct LSGA at different border types remain unknown to date. It has been proposed that sub-RPE deposits, in particular basal laminar deposits (BLamD), are the histologic correlate of the hyporreflective material observed between the two parts of RPE/BM-complex on SD-OCT in the 'splitting' border type.[18] In one clinicopathological correlation study, Sarks et al.[35] correlated the excessive accumulation of BLamD with funduscopically visible hyperpigmentation, which are key feature of the 'diffuse-trickling' FAF phenotype with its high proportion of 'splitting' borders.[18,36] Based on this observation, it has been speculated that basal deposits lead by increasing thickening and separation of the RPE from the choroidal blood supply, and subsequently to RPE and photoreceptor degeneration (summarized in Ref. 35). The high values for LSGA observed among 'splitting' borders would fit well into these hypotheses. Of note, BLamD are not exclusive to 'diffuse-trickling' GA, rather they can be found in the majority of eyes with GA and even normal fundi.[35] They may just be outstandingly thick at the border of 'diffuse-trickling' GA so they become representable by SD-OCT.[18] If local differences in accumulation of sub-RPE material were responsible for locally distinct local atrophy progression kinetics this could represent a novel therapeutic target that should be addressed. Perspectively, under this assumption, it would be interesting to investigate if there is a linear correlation between the thickness of those BLamD and local atrophy progression in future.

Within this work a mean lateral progression of the respective atrophic lesion (LSGA) of 117.86 ± 9.19 μm/y was observed. This value is within the range of findings

reported by Schatz and McDonald[37] on fundus photography (mean: 139 μm/y range, 15–375 μm), and is in line with our recent data based on SD-OCT image analysis (median: 106.90 μm/y, IQR, 55.44–161.70).[17] The particularly faster LSGA of 'splitting' borders is also in accordance with previous observations: Moussa et al.[23] revealed that the presence of the 'splitting' at the nasal and/or temporal border of an atrophic lesion was associated with an faster overall atrophy progression as measured on FAF images. Of note, in that work only overall and not local progression was assessed. Yet, the fact that the observation of a single atrophy border of the 'splitting' type was already associated with a faster overall GA progression suggests that either border types must be highly homogeneous within a single eye or the 'splitting' border must exhibit a very robust effect on atrophy progression. The present results showed that 49% of the eyes exhibited more than one border type. Yet, in a mixed-effects model that took account for eye and patient specific factors, LSGA in 'splitting' borders was still 2- to 3-fold faster than in other border types. The 'splitting' border type has been initially described in a particularly fast progressing GA phenotype, termed 'diffuse-trickling'.[18] In accordance with previous publications[23] these data show that the 'splitting' type borders are by no means exclusive to 'diffuse-trickling' GA. Yet, they are significantly more frequent in 'diffuse-trickling' GA as compared with 'non-diffuse-trickling' GA.

It is of particular interest that the relationship between border type and LSGA maintained statistical significance even when including the FAF phenotype into the model. Although further research and even higher case numbers will be required to draw robust conclusions, this could mean that much of the differences in atrophy progression observed between distinct FAF phenotypes can additionally be explained by distinct proportions of the different OCT border types.

Progression at four defined atrophy borders (superior, nasal, inferior, and temporal) was assessed in horizontal and vertical high-resolution SD-OCT scans with improved signal-to-noise ratio obtained by averaging of multiple images. Obviously, these four borders may not be representative for the entire lesion, which represents a limitation in this analysis. As the present work addresses the relationship between border type and atrophy progression at the very same location, a volumetric assessment is not necessary per se. Still, the impact of the observed differences for the overall function of an individual eye would be assessed more holistic by a volumetric dataset. To perform such analyses in future en face SD-OCT images, derived from slabs encompassing the outer retinal bands will be helpful. Approaches for slab generation may be parallel to those used by Nunes et al.[21] and Niu et al.[25] The latter study presented a predictive model for local GA progression that was based on the thicknesses of various retinal layers and local reflectivity values. Remarkably, in that model—though developed only on a limited number of eyes—the thickness of the RPE–BM complex was one important predictor for atrophy progressions. This observation is well in line with the results presented herein.

The key limitation of addressing only single B-scans instead of volumetric data is that the angle in which the analyzed B-scan cuts the atrophy border strongly influences the measured local atrophy progression according to the laws of trigonometry. As there is no reason why a particular atrophy border type or a border location should be systematically cut by B-scans in a different angle we believe that this will have overall lead to an increased variance in our dataset. Therefore, the significantly faster LSGA in 'splitting' borders is assumed to be real. Instead, it is rather the question if there is really no true difference in LSGA between 'regular' and 'irregular' borders and statistical significance was lost due to the described trigonometric problem. Noteworthy, we used the 'high-speed' mode to acquire SD-OCT scans. Using the 'high-resolution' mode (doubling the lateral resolution) could have provided additional details, increasing the certainty when grading atrophy borders.

In summary, the results indicate that SD-OCT–based assessment of local GA border morphology may serve as predictor for local atrophy progression. In particular, an atrophy border characterized by a splitting of the RPE–BM complex is associated with significantly faster atrophy progression as compared with other border types. These data help to better understand the natural history and pathogenetic factors of GA. Assessment of the SD-OCT border type will allow for better prognostic assessment of the individual eye and identification of the 'splitting' border type as morphologic risk characteristic may disclose a new therapeutic target.

Acknowledgments

The authors thank Ulrich Mansmann and Christine Adrion for discussing the biostatistical workup.

Supported by the German Research Foundation (DFG; Bonn, Germany), Grant No FL658/4-1 and FL658/4-2 (MF) and LI2846/1-1 (ML); and the BONFOR GEROK Program, Faculty of Medicine, University of Bonn, Grant No O-137.0022 and O-137.0025 (MP; Bonn, Germany); ML is the Knoop Junior Research Fellow at St. Cross College, Oxford, UK.

Disclosure: **M. Lindner**, Carl Zeiss Meditec (F, I), Genentech (F), Heidelberg Engineering (F), Optos (F), Fresenius Medical Care (I), Allergan (R), Alimera Sciences (R); **S. Kosanetzky**, Carl Zeiss Meditec (F), Heidelberg Engineering (F), Optos (F); **M. Pfau**, Carl Zeiss Meditec (F), Heidelberg Engineering (F), Optos (F), Bayer Healthcare (R); **J. Nadal**, None; **L.A. Gördt**, Carl Zeiss Meditec (F), Heidelberg Engineering (F), Optos (F); **S. Schmitz-Valckenberg**, Novartis (C, F), Allergan (F), Bayer Healthcare (F, R), Carl Zeiss Meditec (F), Formycon (F), Genentech (F), Heidelberg Engineering (F, R), Optos (F); **M. Schmid**, None; **F.G. Holz**, Acucela (C, F), Allergan (F, R), Bayer (C, F, R), Bioeq (C, F), Genentech/Roche (C, F, R), NightstarX (F), Novartis (C, F, R), Heidelberg Engineering (C, F, R), Optos (F), Pixium (F), Zeiss (F, R), Boehringer-Ingelheim, (C), Merz (C), Thea (C); **M. Fleckenstein**, Carl Zeiss Meditec (F), Genentech (F, R), Heidelberg Engineering (F, R), Optos (F), Merz (C), Bayer Healthcare (R), Novartis (R), P

References

1. Gass JD. Drusen and disciform macular detachment and degeneration. *Arch Ophthalmol*. 1973;90:206–217.
2. Lim LS, Mitchell P, Seddon JM, Holz FG, Wong TY. Age-related macular degeneration. *Lancet*. 2012;379:1728–1738.
3. Schmitz-Valckenberg S, Sadda S, Staurenghi G, Chew E, Fleckenstein M, Holz FG; for the Classification of Atrophy Meeting Group. Geographic atrophy: semantic considerations and literature review. *Retina*. 2016;36:2250–2264.
4. Klein R, Klein BE, Franke T. The relationship of cardiovascular disease and its risk factors to age-related maculopathy. The Beaver Dam Eye Study. *Ophthalmology*. 1993;100:406–414.
5. Vingerling JR, Dielemans I, Hofman A, et al. The prevalence of age-related maculopathy in the Rotterdam Study. *Ophthalmology*. 1995;102:205–210.
6. Klein R, Klein BE, Knudtson MD, Meuer SM, Swift M, Gangnon RE. Fifteen-year cumulative incidence of age-related macular degeneration: the Beaver Dam Eye Study. *Ophthalmology*. 2007;114:253–262.
7. Congdon N, O'Colmain B, Klaver CC, et al. Causes and prevalence of visual impairment among adults in the United States. *Arch Ophthalmol*. 2004;122:477–485.

8. Resnikoff S, Pascolini D, Etya'ale D, et al. Global data on visual impairment in the year 2002. *Bull World Health Organ*. 2004; 82:844–851.
9. Brandl C, Stark KJ, Wintergerst M, Heinemann M, Heid IM, Finger RP. Epidemiology of age-related macular degeneration [in German]. *Ophthalmologe*. 2016;113:735–745.
10. Holz FG, Strauss EC, Schmitz-Valckenberg S, van Lookeren Campagne M. Geographic atrophy: clinical features and potential therapeutic approaches. *Ophthalmology*. 2014; 121:1079–1091.
11. Green WR, Key SN III. Senile macular degeneration: a histopathologic study. *Trans Am Ophthalmol Soc*. 1977;75: 180–254.
12. Sarks JP, Sarks SH, Killingsworth MC. Evolution of geographic atrophy of the retinal pigment epithelium. *Eye (Lond)*. 1988; 2(Pt 5):552–577.
13. Drexler W. Ultrahigh-resolution optical coherence tomography. *J Biomed Opt*. 2004;9:47–74.
14. Staurenghi G, Sadda S, Chakravarthy U, Spaide RF. Proposed lexicon for anatomic landmarks in normal posterior segment spectral-domain optical coherence tomography: the IN*OCT consensus. *Ophthalmology*. 2014;121:1572–1578.
15. Fleckenstein M, Wolf-Schnurrbusch U, Wolf S, von Strachwitz C, Holz FG, Schmitz-Valckenberg S. Imaging diagostics of geographic atrophy [in German]. *Ophthalmologe*. 2010;107: 1007–1015.
16. Fleckenstein M, Charbel Issa P, Helb HM, et al. High-resolution spectral domain-OCT imaging in geographic atrophy associated with age-related macular degeneration. *Invest Ophthalmol Vis Sci*. 2008;49:4137–4144.
17. Fleckenstein M, Schmitz-Valckenberg S, Adrion C, et al. Tracking progression with spectral-domain optical coherence tomography in geographic atrophy caused by age-related macular degeneration. *Invest Ophthalmol Vis Sci*. 2010;51: 3846–3852.
18. Fleckenstein M, Schmitz-Valckenberg S, Martens C, et al. Fundus autofluorescence and spectral-domain optical coherence tomography characteristics in a rapidly progressing form of geographic atrophy. *Invest Ophthalmol Vis Sci*. 2011;52: 3761–3766.
19. Brar M, Kozak I, Cheng L, et al. Correlation between spectral-domain optical coherence tomography and fundus autofluorescence at the margins of geographic atrophy. *Am J Ophthalmol*. 2009;148:439–444.
20. Stetson PF, Yehoshua Z, Garcia Filho CA, Portella Nunes R, Gregori G, Rosenfeld PJ. OCT minimum intensity as a predictor of geographic atrophy enlargement. *Invest Ophthalmol Vis Sci*. 2014;55:792–800.
21. Nunes RP, Gregori G, Yehoshua Z, et al. Predicting the progression of geographic atrophy in age-related macular degeneration with SD-OCT en face imaging of the outer retina. *Ophthalmic Surg Lasers Imaging Retina*. 2013;44: 344–359.
22. Holz FG, Bindewald-Wittich A, Fleckenstein M, Dreyhaupt J, Scholl HP, Schmitz-Valckenberg S. Progression of geographic atrophy and impact of fundus autofluorescence patterns in age-related macular degeneration. *Am J Ophthalmol*. 2007; 143:463–472.
23. Moussa K, Lee JY, Stinnett SS, Jaffe GJ. Spectral domain optical coherence tomography-determined morphologic predictors of age-related macular degeneration-associated geographic atrophy progression. *Retina*. 2013;33:1590–1599.
24. Lindner M, Boker A, Mauschitz MM, et al. Directional kinetics of geographic atrophy progression in age-related macular degeneration with foveal sparing. *Ophthalmology*. 2015;122: 1356–1365.
25. Niu S, de Sisternes L, Chen Q, Rubin DL, Leng T. Fully automated prediction of geographic atrophy growth using quantitative spectral-domain optical coherence tomography biomarkers. *Ophthalmology*. 2016;123:1737–1750.
26. Holz FG, Bindewald-Wittich A, Fleckenstein M, Dreyhaupt J, Scholl H, Schmitz-Valckenberg S. Progression of geographic atrophy and impact of fundus autofluorescence patterns in age-related macular degeneration. *Am J Ophthalmol*. 2007; 143:463–472.
27. Fleckenstein M, Schmitz-Valckenberg S, Adrion C, et al. Progression of age-related geographic atrophy: role of the fellow eye. *Invest Ophthalmol Vis Sci*. 2011;52:6552–6557.
28. Lindner M, Bezatis A, Czauderna J, et al. Choroidal thickness in geographic atrophy secondary to age- related macular degeneration. *Invest Ophthalmol Vis Sci*. 2015;56:875–882.
29. Schmitz-Valckenberg S, Steinberg JS, Fleckenstein M, Visvalingam S, Brinkmann CK, Holz FG. Combined confocal scanning laser ophthalmoscopy and spectral-domain optical coherence tomography imaging of reticular drusen associated with age-related macular degeneration. *Ophthalmology*. 2010;117:1169–1176.
30. Helb HM, Charbel Issa P, Fleckenstein M, et al. Clinical evaluation of simultaneous confocal scanning laser ophthalmoscopy imaging combined with high-resolution, spectral-domain optical coherence tomography. *Acta Ophthalmol*. 2010;88:842–849.
31. Schmitz-Valckenberg S, Fleckenstein M, Gobel AP, Hohman TC, Holz FG. Optical coherence tomography and autofluorescence findings in areas with geographic atrophy due to age-related macular degeneration. *Invest Ophthalmol Vis Sci*. 2011;52:1–6.
32. Bindewald A, Schmitz-Valckenberg S, Jorzik JJ, et al. Classification of abnormal fundus autofluorescence patterns in the junctional zone of geographic atrophy in patients with age related macular degeneration. *Br J Ophthalmol*. 2005;89: 874–878.
33. R Development Core Team. *A Language and Environment for Statistical Computing*. Vienna: R Foundation for Statistical Computing; 2012.
34. Dreyhaupt J, Mansmann U, Pritsch M, Dolar-Szczasny J, Bindewald A, Holz FG. Modelling the natural history of geographic atrophy in patients with age-related macular degeneration. *Ophthalmic Epidemiol*. 2005;12:353–362.
35. Sarks S, Cherepanoff S, Killingsworth M, Sarks J. Relationship of Basal laminar deposit and membranous debris to the clinical presentation of early age-related macular degeneration. *Invest Ophthalmol Vis Sci*. 2007;48:968–977.
36. Fleckenstein M, Schmitz-Valckenberg S, Lindner M, et al. The "diffuse-trickling" fundus autofluorescence phenotype in geographic atrophy. *Invest Ophthalmol Vis Sci*. 2014;55: 2911–2920.
37. Schatz H, McDonald HR. Atrophic macular degeneration. Rate of spread of geographic atrophy and visual loss. *Ophthalmology*. 1989;96:1541–1551.

APPENDIX

Centers and Members That Participated in the FAM Study

Department of Ophthalmology, University of Bonn, Germany: Frank G. Holz, Steffen Schmitz-Valckenberg, Monika Fleckenstein, Moritz Lindner, Julia Steinberg, Maximilian Pfau, Joanna Czauderna.

Institute of Biostatistics, University of Bonn, Germany: Matthias Schmid, Rolf Fimmers, Jennifer Nadal.

Department of Ophthalmology, University of Aachen, Germany: Peter Walter, Andreas Weinberger.

Department of Ophthalmology, Inselspital, University of Bern, Switzerland: Sebastian Wolf, Ute Wolf-Schnurrbusch.

Department of Ophthalmology, University of Heidelberg, Germany: Hans E. Völcker, Friederike Mackensen.

Department of Ophthalmology, University of Leipzig, Germany: Peter Wiedemann, Andreas Mössner.

Department of Ophthalmology, St. Franziskus Hospital Münster, Germany: Daniel Pauleikhoff, Georg Spital.

Institute of Human Genetics, University of Regensburg, Germany: Bernhard H. F. Weber.

Department of Ophthalmology, University of Würzburg, Germany: Claudia von Strachwitz.

Investigative Ophthalmology & Visual Science